Published in final edited form as:

Biomaterials. 2015 December ; 73: 1–11. doi:10.1016/j.biomaterials.2015.09.001.

Hyaluronic Acid-Serum Hydrogels Rapidly Restore Metabolism of Encapsulated Stem Cells and Promote Engraftment

Angel T. Chan, MD, PhD[*], **Mehmet F. Karakas, MD**[*], **Styliani Vakrou, MD**[*], **Junaid Afzal, MBBS, MS**[*], **Andrew Rittenbach, MS**[¥], **Xiaoping Lin, MD, PhD**[*], **Richard L. Wahl, MD**[¥], **Martin G. Pomper, MD, PhD**[¥], **Charles J. Steenbergen, MD, PhD**[†], **Benjamin M.W. Tsui, PhD**[¥], **Jennifer H. Elisseeff, PhD**[+], and **M. Roselle Abraham, MD**[*]

[*]Department of Medicine, Johns Hopkins University, Baltimore, MD

[+]Department of Biomedical Engineering, Johns Hopkins University, Baltimore, MD

[¥]Department of Radiology, Johns Hopkins University, Baltimore, MD

[†]Department of Pathology, Johns Hopkins University, Baltimore, MD

Abstract

Background—Cell death due to anoikis, necrosis and cell egress from transplantation sites limits functional benefits of cellular cardiomyoplasty. Cell dissociation and suspension, which are a pre-requisite for most cell transplantation studies, lead to depression of cellular metabolism and anoikis, which contribute to low engraftment.

Objective—We tissue engineered scaffolds with the goal of rapidly restoring metabolism, promoting viability, proliferation and engraftment of encapsulated stem cells.

Methods—The carboxyl groups of HA were functionalized with N-hydroxysuccinimide (NHS) to yield HA succinimidyl succinate (HA-NHS) groups that react with free amine groups to form amide bonds. HA-NHS was cross-linked by serum to generate HA:Serum (HA:Ser) hydrogels. Physical properties of HA:Ser hydrogels were measured. Effect of encapsulating cardiosphere-derived cells (CDCs) in HA:Ser hydrogels on viability, proliferation, glucose uptake and metabolism was assessed in vitro. In vivo acute intra-myocardial cell retention of ^{18}FDG-labeled CDCs encapsulated in HA:Ser hydrogels was quantified. Effect of CDC encapsulation in HA:Ser hydrogels on in vivo metabolism and engraftment at 7 days was assessed by serial, dual isotope SPECT-CT and bioluminescence imaging of CDCs expressing the Na-iodide symporter and firefly luciferase genes respectively. Effect of HA:Ser hydrogels +/− CDCs on cardiac function was assessed at 7 days & 28 days post-infarct.

Results—HA:Ser hydrogels are highly bio-adhesive, biodegradable, promote rapid cell adhesion, glucose uptake and restore bioenergetics of encapsulated cells within 1 h of encapsulation, both in vitro and in vivo. These metabolic scaffolds can be applied epicardially as a patch to beating hearts or injected intramyocardially. HA:Ser hydrogels markedly increase acute intramyocardial retention

(~6 fold), promote in vivo viability, proliferation, engraftment of encapsulated stem cells and angiogenesis.

Conclusion—HA:Ser hydrogels serve as 'synthetic stem cell niches' that rapidly restore metabolism of encapsulated stem cells, promote stem cell engraftment and angiogenesis. These first ever, tissue engineered metabolic scaffolds hold promise for clinical translation in conjunction with CDCs and possibly other stem cell types.

Keywords

HA:Serum hydrogels; stem cells; metabolism; molecular imaging; angiogenesis; engraftment

Introduction

Stem cell therapy offers the promise of organ repair on demand. Experimental and clinical studies indicate small improvements in heart function, which are often not sustained over the long run. An important obstacle to sustained functional benefits is very low levels of acute stem cell retention and engraftment. We have previously demonstrated[1] using cardiosphere-derived cells (CDCs)[2] that dissociation leads to rapid depression of stem cell bioenergetics, indicating a relationship between cellular metabolism and adhesion. Molecular imaging studies using micro-PET/CT of ex vivo ^{18}FDG-labeled CDCs reveal that ~80% of injected CDCs are lost into the lungs and systemic circulation in the first hour following intra-myocardial transplantation[3]. These results have motivated us to design scaffolds that boost acute myocardial retention and promote rapid restoration of transplanted cell bioenergetics.

Currently, most clinical and experimental cell therapy protocols in the heart utilize direct injection of isolated cells, resulting in low levels of acute myocardial retention as well as massive cell death (anoikis, necrosis) due to lack of cell-cell or cell-ECM (extracellular matrix) contact[4], and lack of substrates. We have designed autologous, biodegradable, bio-adhesive, hydrophilic scaffolds (hydrogels) that combine serum and hyaluronic acid (HA). We chose serum (which is an important component of cell culture medium) because it can provide substrates/growth factors needed for stem cell survival/proliferation. Furthermore, immobilization of serum in hydrogels can provide RGD (Arg-Gly-Asp) motifs in vitronectin and fibronectin (which are components of serum)[5, 6] for cell adhesion (integrin activation) [7]. HA is one of the chief components of cardiac extracellular matrix, has been demonstrated to provide a microenvironment for self-renewal, differentiation of stem cells[8] and is implicated in cell adhesion and motility [8–10]. The degradation products of HA also promote angiogenesis[8], which could promote transplanted cell engraftment and cardiac regeneration.

In this study, the carboxyl groups of HA were modified with N-hydroxysuccinimide (NHS) to yield HA-NHS groups which react with free amine groups present on serum proteins and tissue to form amide bonds, resulting in hydrogels that encapsulate stem cells and adhere to transplanted tissue. HA:Ser hydrogels polymerize when HA-NHS and serum are mixed, can be applied epicardially (as a patch) to beating hearts or delivered by intra-myocardial injection with high levels of acute retention (70–100%). Our novel result is that HA:Ser

hydrogels promote restoration of cellular bioenergetics within 1 h of encapsulation, both in vitro and in vivo by promoting rapid cell adhesion.

Materials and Methods

Modification of Hyaluronic Acid—Chemical modification of carboxyl groups in hyaluronic acid (HA) to amine-reactive N-hydroxysuccinimide esters was achieved by reacting 10%(w/v) HA (MW 16 kDa; LifeCore Biomedical) with 67%(w/v) 1-ethyl-3-(3-diemthylaminopropyl) carbodiimide (EDC; Sigma) and 25%(w/v) N-hydroxyl succinimide (NHS; Sigma) in phosphate-buffered saline (PBS) as previously described [11, 12]. The hydroxamate assay[11] revealed that 36±0.8% of the carboxylic acid groups in HA formed sulfo-NHS-esters. The -NHS groups from HA hydrolyzed within 10 min with amide bond formation between carboxylic acid groups in HA and amine groups.

Hydrogel Synthesis—HA:Ser hydrogels were synthesized by chemical crosslinking of –NHS with amine groups present on serum proteins. Specifically, 10%(w/v) HA-NHS dissolved in PBS or IMDM (containing 25gm/L glucose) was mixed with an equal volume of serum (from syngeneic WK rats) in a 1:1 (v/v) ratio, at room temperature for 5min. We chose a 1:1 (v/v) ratio for serum and HA in order to maximize adhesivity and supply of adhesion motifs/growth factors present in serum. In order to ensure functionality of -NHS groups, hydrogels were synthesized within 5 min of dissolving HA-NHS in PBS. HA:PEG hydrogels were prepared by mixing in a 1:1 (v/v) ratio, 10%(w/v) HA-NHS in PBS and 10% (w/v) PEG-$(NH_2)_6$ in HEPES buffer at room temperature and pH 7-7.4[11].

For in vitro cell proliferation studies, stem cells were suspended in serum and subsequently mixed with HA-NHS (dissolved in PBS) in a 1:1 (v/v) ratio, and cultured in cell–specific culture medium which ensured availability of optimal concentrations of substrates/growth factors to encapsulated stem cells. For in vivo studies, HA-NHS dissolved in IMDM (Invitrogen) and CDCs suspended in serum were each aspirated into separate sterile 0.5 mL syringes connected by sterile plastic tubing. HA-NHS and serum were mixed immediately prior to intra-myocardial injection or epicardial application. Since IMDM is used to culture CDCs in vitro, IMDM which contains 25 mM glucose was used to dissolve HA-NHS for in vivo studies -this ensured availability of glucose to encapsulated CDCs following transplantation.

Measurement of Physical Properties of HA:Ser hydrogels—Hydrogels were prepared as cylindrical blocks, 5 mm in diameter, with a total volume of 50 or 100 μL containing 1:1 (v/v) ratio of 10%(w/v) HA-NHS in PBS and serum, using caps of microcentrifuge tubes as molds. Mechanical and physical properties of HA:Ser hydrogels were characterized by measuring swelling ratio, gelation time, compressive modulus, degradation rate and protein releas [11].

Equilibrium swelling ratio analysis[11]: HA:Ser hydrogels were incubated in PBS overnight in order to measure their wet weight at maximum saturation. They were subsequently transferred to pre-weighed microcentrifuge tubes and lyophilized for 48 h in

order to measure dry weight. The ratio of wet to dry weight was determined as the swelling ratio of the hydrogels.

Gelation time analysis[11]: Using a 2–200 μL pipetman, HA-NHS and serum were mixed and pipetted up and down until the solutions could no longer be pipetted. The time at which this happened was designated as the gelation time.

Compressive (Young's) modulus analysis[11]: To measure compressive modulus, hydrogel constructs were placed in between two parallel metal plates on an adjustable stage. The bottom plate was attached to a 250g loading weight and a force transducer, connected to a computer. The gels were then deformed by 1% height in discrete 20sec intervals until 10% deformation was reached (electroforce 3200 testing instrument, Bose). The best fit slope of the stress-strain curve (4–9% strain) was used to calculate compressive modulus.

Degradation rate[11]: Hydrogels can be degraded by hydrolysis, proteases present in tissue and/or secreted by encapsulated CDCs. Since cells can secrete matrix metalloproteinases and hyaluronidases which could accelerate degradation of hydrogels, studies of hydrogel degradation were performed with and without encapsulated cells. Hydrogel constructs (50 μL) without cells (n=3) and hydrogels containing encapsulated CDCs (n=5) were incubated in culture medium at 37 °C for 12 days; hydrogel dry weights were measured every 4 days. Change in gel dry weight was used to quantify degradation rate.

Protein release from HA:Ser hydrogels: Soluble serum proteins from HA:Ser hydrogels can be released over time. In order to assess protein release, HA:Ser hydrogels (50 μL volume; n=3) were incubated in PBS at 37 °C. Sample aliquots (5–40 μL of PBS solution) were obtained over 20 days and protein concentration was measured using the Bradford assay (BioRad). The total volume of PBS was readjusted to 1 mL after each sampling. Total serum protein concentration was determined from 25 μL of serum suspended in 1 mL PBS (equivalent to the hydrogel) in order to normalize results of protein estimation to the total protein content of serum.

Stem Cells

Cardiosphere-derived cells (CDCs) were used for all in vitro and in vivo studies. CDCs are comprised of mixtures of cell populations[13] that express markers of cardiac progenitor cells (c-kit$^+$/CD90$^-$), mesenchymal stem cells (c-kit$^-$/CD105$^+$, CD90$^+$) and endothelial cells (c-kit$^-$/CD34$^+$), that together, have a synergistic effect on cardiac regeneration[14, 15]. CDCs[2] are currently in Phase 2 Clinical trials (ALLSTAR) for treatment of patients following myocardial infarction and in Phase 1 clinical trials (DYNAMIC) for treatment of patients with dilated cardiomyopathy. For this study, CDCs were isolated from hearts of male, 5 weeks old Wistar Kyoto (syngeneic) rats (Charles Rivers) as previously described[13]. CDCs were cultured and expanded in cardiac explant medium (CEM), composed of IMDM (Invitrogen), 10% fetal bovine serum (FBS), 1% L-Glutamine, and 0.05 mM 2-mercaptoethanol in non-coated flasks.

Human mesenchymal stem cells (MSCs) derived from bone marrow, were purchased from Millipore (Cat. No. SCR108). MSCs were cultured and expanded in Dulbecco's modified

Eagle medium (DMEM), 10% FBS, 1% L-Glutamine, 0.05 mM 2-mercaptoethanol and 8 ng/mL of FGF-2 using instructions from the manufacturer.

Mouse embryonic stem cells (syNP4 cell line kindly supplied by Dr. Kenneth Boheler) were cultured in Glasgow minimum essential medium (GMEM) supplemented with 10% FBS, 1% glutamax, 1 mM sodium pyruvate, 1% minimum essential medium-non-essential amino acid, 0.1 mM 2-mercaptoethanol, and 10^6 units of leukemia inhibitory factor.

Lentivirus synthesis—A third-generation lentiviral vector system (kindly supplied by Professor Inder Verma, Salk Institute) was used to label CDCs. The cDNA encoding the hNIS (human sodium iodide symporter) gene or the cDNA pGL4.10[luc2] encoding firefly luciferase (Promega) was sub-cloned in place of eGFP into the vector RRLsin18.cPPT.CMV.eGFP.Wpre, resulting in plasmids designated cpPPT.CMV.hNIS or pPPT.CMV.fLuc as previously described[1]. Viral vectors were produced and titered as described previously[1]. For genetic labeling, rat CDCs were transduced at a multiplicity of infection (MOI) of 20, yielding transduction efficiencies of >70% for hNIS expression and >90% for fLuc expression. NIS expression was confirmed by immunostaining using a monoclonal mouse anti-hNIS antibody (Abcam) and by in vitro ^{99m}Tc-pertechnetate uptake, while luciferase expression was examined by immunostaining using a polyclonal goat anti-luciferase antibody (Promega) and by an in vitro bioluminescence assay. We have previously demonstrated that transduction of CDCs with firefly luciferase or hNIS at an MOI of 20 does not affect cell proliferation, using in vitro studies.[3, 16]

Two Photon microscopy—Live cell imaging was performed using the FV1000 2-photon microscope (Olympus), excitation wavelength of 780 nm and 25X water lens using identical laser power, gain and zoom. Images of 512×512 pixels were collected up to 200 μm depth and digitized at 8-bit resolution. Image analysis was performed using identical parameters for all conditions, using ImageJ (NIH, http://rsb.info.nih.gov/ij/). Chinese hamster ovary (CHO) cells expressing α_4 integrin fused to eGFP were used to assess status of integrin activation following encapsulation in HA:Ser and HA:PEG hydrogels. CHO cells were trypsinized and either suspended in PBS for 1 h, encapsulated in HA:Ser or HA:PEG hydrogels or plated as monolayers. Two-photon imaging was performed at 1 h post-plating/encapsulation.

In vitro Stem Cell Viability and Proliferation—For in vitro studies, CDCs, MSCs or ESCs were suspended in serum at a concentration of 10,000 cells/μL of hydrogel for all experiments.

Cell Viability: The Live/Dead viability assay (Molecular Probes) was used to assess cell viability. The principle is as follows: Calcein is a cytoplasmic dye that is taken up and cleaved by cytoplasmic esterases, staining the cytoplasm of viable cells green; Ethidium homodimer-1 is used to identify cells undergoing cell death because it is a nuclear stain that only permeates cells with compromised cell membranes, staining the nucleus red. Cells were labeled with calcein (2 μM) and Ethidium homodimer-1 (2 μM) for 20 min. The samples were then washed with PBS twice, immersed in culture medium, and imaged using 2-photon microscope.

Cell Proliferation: After culturing each cell type (CDCs, MSCs, or ESCs) encapsulated in HA:Ser or HA:PEG hydrogels (n=3 for each) in cell-specific medium for d0, d4 and d8 (days), samples were lyophilized for 48 h and digested with 500 μL proteinase K (0.1 mg/mL proteinase K, 10 mM Tris, 1 mM EDTA, and 0.1% Triton X-100) at 50 °C for 24 h. An aliquot (5 μL) was used to quantify double-stranded DNA concentration using the PicoGreen assay (Invitrogen). Since nuclei from lysed blood cells can produce a signal, results were normalized to the signal obtained at the time of cell encapsulation (d0) to determine percentage change from the baseline. PicoGreen is a flurochrome that selectively binds dsDNA and has an excitation/emission maxima at 480/520 nm. When bound to dsDNA, its fluorescence enhancement is exceptionally high; little background occurs since the unbound dye has virtually no fluorescence[17].

Growth (paracrine) factor expression—CDCs were cultured as monolayers in medium containing FBS (fetal bovine serum) or encapsulated in HA:Ser hydrogels composed of HA-NHS cross-linked by FBS for 48 h. Subsequently, hydrogels were homogenized and mRNA was isolated according to the manufacturer's instructions (RNeasy mini kit; Qiagen). Real time PCR was performed using SYBR® Green and iCycler (BioRad; Applied Biosystems). Insulin-like growth factor (IGF-1), hepatocyte growth factor (HGF), and vascular endothelial growth factor (VEGF) were targeted because they are secreted by CDCs[18] and are involved in cardiac regeneration[19]. The following rat-specific forward primers were used: IGF: 5′-GACGCTCTTCAGTTCGTG TGT-3′, HGF 5′-AGCCATGTACGTAGCCATCC-3′, and VEGF 5′-GGTAATGGCTCCTCCTCCTC-3′.

In vitro investigation of CDC metabolism—Radiotracer uptake (^{18}FDG, ^{99m}Tc-pertechnetate) rather than in vitro BLI was used to assess cellular bioenergetics, because hydrogels induce attenuation of the BLI signal which precludes comparison of encapsulated CDCs with non-encapsulated adherent/suspended fLuc^{+}CDCs. The following conditions were investigated: Suspension, adherent/monolayer, hydrogel encapsulation of CDCs for 1, 3 and/or 24 h. For suspension culture, culture plates were coated with Polyhydroxyethylmethacrylate (Poly-HEMA 12 mg/mL). Single cell suspensions were achieved by the addition of 1 mM EDTA which prevents formation cell clumps, to cell culture medium.

In vitro Glucose (^{18}FDG) uptake: CDCs were plated for 1, 3 or 24 h on Poly-HEMA-coated 6 well plates for the suspension condition, on regular tissue culture-treated 6 well plates for the monolayer condition or encapsulated in hydrogels. Prior to labeling, cells were washed twice with PBS and the medium was changed to glucose free-DMEM for 1 h. Cells were radio-labeled by incubating with 74 kBq/mL of ^{18}FDG in glucose-free DMEM containing 10% FBS for 1 h, immediately after, 2 h or 23 h after generation of cell suspensions, plating as monolayers or encapsulation in 20 μL hydrogels (15,000 cells/μL) for the 1 h, 3 h and 24 h conditions respectively. Control hydrogels without cells were prepared to measure background radioactivity in hydrogels due to trapping of isotope. Subsequently, cells were washed twice with cold PBS to remove any remaining free ^{18}FDG, lysed with proteinase K solution, and transferred to 20 mL scintillation vials. Counts were recorded in a gamma-counter (Perkin Elmer). After gamma counting, samples were stored at

−20 °C to allow for radiotra cer decay, prior to performing the Pico® Green DNA assay to measure total DNA content. ^{18}FDG uptake was normalized to cell number.

In vitro ^{99m}Tc-Pertechnetate uptake[3, 20]: NIS^{+}CDCs were plated for 1, 3 or 24 h on Poly HEMA-coated 6 well plates for the suspension condition, on regular tissue culture-treated 6 well plates for the monolayer condition or encapsulated in hydrogels. NIS^{+}CDCs were radio-labeled by incubating with ^{99m}Tc-pertechnetate (11.1 kBq/mL) in DMEM containing 10% FBS for 1 h, immediately after, 2 h or 23 h after generation of cell suspensions, plating as monolayers or encapsulation in 20 μL hydrogels (15,000 cells/μL) for the 1 h, 3 h and 24 h conditions respectively. The effect of perchlorate, a specific NIS blocker on ^{99m}Tc-pertechnetate uptake was measured by adding 100 μM perchlorate to some wells prior to the addition of ^{99m}Tc-pertechnetate. At the end of 1 h, CDCs/hydrogels were rinsed twice with ice cold PBS and lysed with proteinase K. Counts were recorded in a gamma-counter (Perkin Elmer) and the DNA assay (Quant-iT™ Picogreen DNA Assay-Life Technologies) was performed to normalize the uptake by total DNA (cell) content. ^{99m}Tc-pertechnetate uptake was normalized to cell number.

Respirometry: Seahorse Bioscience XF instrument (XF24 with Islet capture plates)[1, 21] was used to measure oxygen consumption rate (OCR). Respiratory rates were measured as basal rates. Normalization of respiratory rates was performed using a DNA assay (Quant-iT™ Picogreen DNA Assay-Life Technologies).

Animal Studies

In vivo Animal Studies—Since immunologic and inflammatory responses can result in death of transplanted cells and reduce cell retention/engraftment, we 1) used syngeneic Wistar Kyoto rats for CDC/serum isolation and in vivo cell transplantation experiments, and 2) washed CDCs twice in serum-free medium in order to reduce immunologic and inflammatory reactions to transplanted CDCs.

Animal surgery: CDCs derived from male Wistar Kyoto rats were transplanted into syngeneic, female Wistar Kyoto rats (200–250 g or 10–12 weeks old obtained from Charles River), which permitted quantification of transplanted cells, using qPCR for the male-specific SRY gene. Anesthesia was induced with 5% isoflurane flowed in with 2 L/min oxygen, and maintained with 2% isoflurane. The heart was exposed through a left lateral thoracotomy in the 4th and 5th intercostal space. The pericardium was opened. For induction of myocardial infarction, the mid portion of the left anterior descending artery was ligated using a 5-0 silk suture; infarction was confirmed by pallor in the myocardial territory supplied by the ligated portion. Hydrogels +/− CDCs were either injected intramyocardially into 2 sites in the anterior wall/infarcted myocardium or applied epicardially to the anterior wall. For epicardial applications, the epicardium was treated with 2.5% trypsin for 1–2 min, following which hydrogels were applied to the beating heart. Subsequently, the chest was closed using 3-0 silk suture.

In vivo Acute Stem Cell Retention—^{18}FDG–labeled CDCs were used to quantify acute myocardial retention and bio-distribution following intra-myocardial transplantation into

non-infarcted myocardium using methods previously developed by us[20]. We chose non-infarcted myocardium to test effects of HA:Ser hydrogel on myocardial retention because it is associated with very low levels of acute retention (compared to the coronary ligation model) based on our previous bio-distribution study[20]. Here, CDCs were labeled with 74 kBq/mL of ^{18}FDG for 30min, washed with ice cold PBS, and trypsinized: 1×10^6 CDCs were suspended in 50 μL of IMDM for the cell suspension condition or encapsulated in 50 μL HA:Ser hydrogels. Rats (n=35) underwent left thoracotomy under general anesthesia with isoflurane as above. ^{18}FDG-labeled CDCs in suspension or encapsulated in HA:Ser hydrogels were injected intramyocardially directly into the anterior wall at 2 sites using a 27G needle. The chest was closed and the animals were allowed to recover for 1 h prior to sacrifice and harvesting of their heart, lungs, liver, brain, kidney, spleen and blood to measure ^{18}FDG activity using a gamma counter (Perkin Elmer).

Dual isotope SPECT-CT imaging—Here, 3×10^6 NIS$^+$CDCs encapsulated in HA:Ser hydrogels were applied epicardially to the anterior wall of the left ventricle in non-infarcted Wistar Kyoto rats following a left sided thoracotomy. $^{99m}TcO_4^-$ (^{99m}Tc-pertechnetate; 555–740 MBq) and ^{201}TlCl (^{201}Tl-chloride; 37–74 MBq) were injected intravenously via the tail vein immediately after cell transplantation; isoflurane was turned off and the animal was monitored for spontaneous breathing and allowed to fully recover prior to imaging. In vivo dual isotope SPECT imaging was performed 1 h after injection of ^{99m}Tc-pertechnetate and ^{201}TlCl. CT imaging was performed prior to SPECT imaging. Both scans were performed on a small animal SPECT/CT system (X-SPECT-CT from Gamma Medica Inc.) using inhalational isoflurane as the anesthetic agent, administered via a nose cone. Animals were allowed to recover in their cages after completion of imaging on d0. The same rats were re-injected with ^{99m}Tc-pertechnetate (555–740 MBq) and ^{201}TlCl (37–74 MBq) via the tail vein and in vivo dual isotope SPECT-CT imaging was performed 1 h after radiotracer injection on d1, d3, and d7 after HA:Ser hydrogel + CDC transplantation.

Dual Isotope SPECT/CT image acquisition and processing: The SPECT module X-SPECT-CT system is composed of two gamma camera heads each consisting of a pixelated NaI(Tl) with a total area of 125 mm×125 mm, divided into 80×80 number of pixels with 1.56 mm pitch. Low-energy knife-edge pinhole collimators were used with a pinhole aperture of 1 mm diameter and a focal length of 9 cm; a radius-of-rotation of 5.42 cm was used in the SPECT data acquisition. Each camera head acquired 128 projections over a 180-degree range, with an acquisition time of 30 s for each projection for all scans. Data was acquired in list mode and subsequently re-binned into two energy windows (“75 keV +10%/−10%” and “140 keV +10%/−10%”) to obtain separate sets of ^{201}Tl and ^{99m}Tc projections. The ^{99m}Tc and ^{201}Tl projection datasets were reconstructed using a 3D pinhole ordered-subset expectation-maximization (OS-EM) imaging reconstruction algorithm with 8 and 4 updates, respectively with an isotropic reconstructed image voxel size of 0.7 mm.

X-ray computed tomography (CT) was performed on the micro-CT module with an X-ray tube voltage of 75 kVp. A total of 512 projections were acquired over a 360-degree range. The projections with 1,184×1,120 isotropic pixels (100 μm) were reconstructed into a CT

volume of 512^3 isotropic voxels with 170 μm pixel size. The SPECT and CT were then registered using rigid body transform, with pre-set parameters specific to the system.

SPECT image quantification: For absolute quantification, a calibration factor (CF) was calculated from an experimental study by inserting a small hollow sphere filled with a known amount of radioactivity of ^{99m}Tc or ^{201}Tl in water in an averaged rat-size water-filled cylindrical phantom to simulate a rat scan. Dose-response plot for ^{99m}Tc-pertechnetate was obtained by dual isotope SPECT imaging of varying doses of ^{99m}Tc-pertechnetate and ^{201}TlCl and then used to calculate the calibration factor. SPECT data for the phantom was acquired using exactly the same acquisition settings as that used in the animal experiments. In this case, the calibration factor or CF (MBq/i.i.) was defined as the quotient of the known activity concentration (MBq/mL) within the radioactive sphere in the phantom divided by the measured mean image intensity (i.i/cm^3) within an ROI drawn over the small sphere in the SPECT image of the phantom.

To quantify tracer uptake in vivo, regions-of-interest (ROI) were manually defined in a region of increased focal tracer uptake and in a contralateral normal region of a mid-myocardial section. In the case of no observable increased focal myocardial tracer accumulation, an ROI was placed in the distal anterior wall. The total radioactivity in the region of interest was calculated by the image intensity within the ROI multiplied by the calibration factor. The radioactivity concentration (MBq/mL) within the ROI was calculated by the total activity divided by volume of the ROI. The background activity was calculated by placing an ROI in the basolateral wall of the heart.

In Vivo Bioluminescence Imaging (BLI)—Previous (unpublished) studies by us reveal higher sensitivity with BLI for cell tracking in vivo. Since intra-myocardial CDC injection is associated with low levels of acute myocardial retention, in vivo BLI was used to examine impact of CDC encapsulation in HA:Ser hydrogels on engraftment following intra-myocardial transplantation. CDCs were transduced with a 3rd generation lentivirus expressing firefly luciferase (Lv-CMV-fLuc) at an MOI of 20, which did not affect CDC survival, proliferation or differentiation[16]. One million fLuc$^+$CDCs were trypsinized, suspended in 50 μL of IMDM (n=3) or encapsulated in 50 μL HA:Ser hydrogels prior to intra-myocardial injection (n=6) into the infarcted territory (using a 27G needle) of Wistar Kyoto rats, immediately following induction of myocardial infarction. In vivo BLI was performed using the Xenogen IVIS 200 system at 1 h (d0), d1, d3 and d7 post-transplantation of fLuc$^+$CDCs or fLuc$^+$CDCs encapsulated in HA:Ser hydrogels.

Image Acquisition and Analysis: Anesthesia was induced using 5% isoflurane in a Plexiglas box. Rats were subsequently transferred to the imaging chamber and anesthesia was maintained using 2% isoflurane administered using a nose cone. D-Luciferin (30 mg/kg in PBS) was injected intraperitoneally and serial imaging was performed every 1 min until peak BLI activity was obtained (20–30 min after injection). An ROI was drawn in the region of the heart to quantify BLI activities at different time points post-transplantation. Since hydrogels can attenuate the BLI signal, the BLI signal obtained on d1, d3 and d7 was normalized to the d0 signal for each group. This precludes direct comparison of engraftment between the 2 groups, but permits longitudinal cell tracking in each group.

Echocardiography—Rats were anesthetized with 1.5% isoflurane (using a nose cone) for the duration of imaging and placed supine on an electrical heating pad; a tensor lamp was used to provide additional heat. The rat core temperature was monitored with a rectal probe. ECG signals were obtained by contacting the rat limbs, coupled with electrically conductive gel to ECG electrodes integrated into the heating pad. Ultrasound imaging was performed using the VEVO 2100 system (Visual Sonics). Using B-mode imaging, the MS250 scan head (f_c=21MHz, 256 elements) was positioned and immobilized using the Visual Sonics Vevo Integrated Rail System. Two dimensional long axis images were used for the measurement of ejection fraction (calculated as the difference between end-diastolic and end-systolic volumes normalized to end-diastolic volume, expressed as a percentage) from parasternal long axis, apical and short axis views as previously described[22].

Quantification of Engraftment by Real Time PCR Analysis—Quantitative PCR was performed on d28 after intra-myocardial injection of 1×10^6 CDCs suspended in 50 μL IMDM and 1×10^6 CDCs encapsulated in 50μl HA:Ser hydrogels to compare engraftment at d28 in these groups. CDCs isolated from male WK rats were injected into female rats; engrafted donor cell numbers were quantified by real-time PCR, using the SRY gene located on the Y chromosome as target.

Whole hearts were weighed, homogenized and genomic DNA was isolated from aliquots of the homogenate corresponding to 12.5 mg of myocardial tissue, using the DNA Easy minikit (Qiagen), according to the manufacturer's protocol. The TaqMan® assay (Applied Biosystems) was used to quantify the number of transplanted cells with the rat SRY gene as template (forward primer: 5′-GGA GAG AGG CAC AAG TTG GC-3′, reverse primer: 5′-TCC CAG CTG CTT GCT GAT C-3′, TaqMan probe: 6FAM CAA CAG AAT CCC AGC ATG CAG AAT TCA G TAMRA, Applied Biosystems)[23]. For absolute quantification of gene copy number, a standard curve was constructed with samples derived from multiple log dilutions of genomic DNA isolated from male rat CDCs. All samples were spiked with 50 ng of female genomic DNA to control for any effects this may have on reaction efficiency in the actual samples. The copy number of the SRY gene at each point of the standard curve is calculated based on the amount of DNA in each sample and the total mass of the rat genome per diploid cell. (http:www.cbs.dtu.dk/databases/DOGS/index.html). All samples were tested in triplicate. For each reaction, 50 ng of template DNA was used. Real time PCR was performed in an ABI PRISM 7700 instrument. The result from each reaction, copies of the SRY gene in 50 ng of genomic DNA, was expressed as the number of engrafted cells/heart, by first calculating the copy number of SRY gene in the total amount of DNA corresponding to 30 mg of myocardium and then extrapolating to the total weight of each heart (since there is one copy of the SRY gene per cell).

Histopathology—Following euthanasia, hearts were fixed in 60%methanol:10%glacial acetic acid mixture for 24 h. Paraffin-embedded heart tissues were sectioned at 6 μm. For immunostaining, high temperature antigen retrieval and paraffin removal was performed by immersing slides in Trilogy (Cell Marque, Hot Springs, AR) in a pressure cooker until the chamber attained a temperature and pressure of 126 °C and 23 psi. Endogenous peroxidase activity was blocked using a 5 min incubation period in 3% H_2O_2 in PBS. Slides were

incubated with a rabbit primary antibody to either von Willibrand factor (Dako Corporation) or alpha smooth muscle actin (Abcam) for 30 min followed by rabbit HRP polymer conjugate (SuperPicTure, Invitrogen) for 10 min. Slides were then stained with Impact DAB (Vector Labs) for 3 min. Sections were counterstained with Hematoxylin (Richard-Allen Scientific)

Statistical Analysis—Continuous variables were expressed as means +/− SE. Intergroup differences were assessed using ANOVA test. P value of <0.05 was considered statistically significant. All statistical analysis was performed using JMP software.

Results

Physical properties of HA:Ser hydrogels

HA:Ser hydrogels were synthesized by chemical crosslinking of –NHS with amine groups present on serum proteins at pH7-7.4. The gelation time of 10%(w/v) HA:Ser hydrogels was 160±30 s which facilitated intra-myocardial injection or epicardial application (Fig 1a) of the cell-hydrogel mixture. Young's (compressive) modulus of 10%(w/v) HA:Ser hydrogels was 5.8±3 kPa, which is similar to rat myocardium during systole (4.2±1.4 kPa)[11]. The swelling ratio of HA:Ser hydrogels was 21.8±1.3 compared to dry gel, which would be expected to permit diffusion of solutes and metabolites into hydrogels.

HA:Ser hydrogels degraded to 57±3% in the absence of encapsulated CDCs and 48±13% in the presence of CDCs (n=3), on d12 post-encapsulation. Degradation of HA:PEG hydrogels was less than HA:Ser hydrogels and similar (90±6%) in the presence/absence of CDCs on d12 post-encapsulation. These results suggest that hydrolysis alone, as in the case of HA:PEG hydrogels leads to slow degradation of hydrogels. HA:Ser hydrogel degradation is accelerated in the presence of cells which may secrete proteases[24] and/or hyaluronidases.

Serum proteins from HA:Ser hydrogels showed a controlled release behavior when incubated in PBS at 37 °C, with a fast release of ~5% of the tot al protein content within the first 6 h of encapsulation (0.8%/h or 44.6 μg/h), followed by slow release phase (0.046%/h or 1.4μg/h) over time (n=3) (Fig 1b). The former fast release phase was likely due to release of unbound or loosely bound protein, and the later release phase was probably secondary to degradation of the scaffold.

HA:Ser hydrogels promote viability and proliferation of encapsulated CDCs, MSCs, ESCs

Using α_4 integrin-eGFP-expressing CHO (Chinese hamster ovary) cells, integrin activation was manifested as membrane localization of integrin, within 1 h following encapsulation in HA:Ser hydrogels (Fig 1c), but not HA:PEG hydrogels, suggesting rapid activation of cell adhesion in HA:Ser hydrogels. Viability was similar (99%) in the 3 cell lines at 1 h post-encapsulation in HA:Ser and HA:PEG hydrogels. Differences in cell proliferation between HA:Ser and HA:PEG hydrogels were evident on d4 and d8 following stem cell encapsulation: proliferation of all three cell lines was high at d4 and d8 in HA:Ser hydrogels. In contrast, encapsulation in HA:PEG hydrogels was associated with reduction in cell number in all 3 cell lines on d4 and evidence of proliferation on d8 in CDCs and ESCs, but not MSCs (Fig 1d).

Encapsulation in HA:Ser hydrogels positively influenced expression of IGF, HGF and VEGF in encapsulated CDCs: 2.5 fold higher expression of IGF, 4.8 fold higher expression of VEGF and 18 fold higher expression of HGF were observed in CDCs encapsulated in HA:Ser hydrogels, compared to CDCs grown as monolayers (n=3, $p<0.001$) (Fig 1e).

HA:Ser hydrogels rapidly restore metabolism of encapsulated CDCs in vitro and in vivo

We have previously demonstrated that cell dissociation and suspension rapidly down regulate glucose uptake, metabolism and ATP levels[1]; suspension also predisposes cells to anoikis[25, 26]. Stem cells utilize glucose as their main energy source[27]. The glucose analog, ^{18}FDG is taken up by glucose transporters, but cannot be degraded by metabolic pathways[28]. In suspended CDCs, glucose (^{18}FDG) uptake progressively decreased over time in suspension, whereas glucose uptake increased over time when CDCs were plated as monolayers or encapsulated in HA:Ser hydrogels (Fig 2a). Notably, glucose uptake was markedly higher in HA:Ser hydrogels at 1, 3 and 24 h, when compared to cells plated as monolayers or suspended cells ($p<0.005$). Interestingly, ^{18}FDG uptake at 1 h following encapsulation in HA:Ser hydrogels was similar to ^{18}FDG uptake in monolayers at 24 h post-plating, indicating rapid restoration of cellular glucose uptake following encapsulation in HA:Ser hydrogels.

Respirometry studies revealed low oxygen consumption rate (OCR) in suspension and ~3 fold increase within 1 h of encapsulation in HA:Ser hydrogels (Fig 2b). Notably, OCR of cells encapsulated in HA:Ser hydrogels for 1 h was significantly higher than cells plated as monolayers for 24 h (Fig 2b), confirming hydrogel-mediated rapid restoration of metabolism in encapsulated cells.

In order to assess impact of cell encapsulation in HA:Ser hydrogels on bioenergetics, CDCs were genetically modified to express NIS which simultaneously transports ^{99m}Tc-pertechnetate and Na^+ into cells – this transport is coupled to Na^+/K^+-ATPase function, which requires ATP (Fig 2c). ^{99m}Tc-pertechnectate was very low in suspended cells and markedly increased following plating as monolayers or encapsulation in hydrogels (Fig 2d). Of note, CDC encapsulation in HA:Ser hydrogels resulted in significantly higher ^{99m}Tc-pertechnetate (33±4 vs. 1.7±0.5 Bq/μg of DNA) at 1 h following encapsulation, when compared to cells plated as monolayers ($p<0.001$) for 24 h, confirming that HA:Ser hydrogels provide a microenvironment that is conducive to rapid restoration of cellular bioenergetics.

In vivo dual isotope SPECT-CT imaging was performed to assess effects of CDC encapsulation on in vivo bioenergetics at 1–3 h post-transplantation: ^{99m}Tc-pertechnectate uptake was very low following transplantation of suspended NIS^+-CDCs (historic controls). In contrast, high ^{99m}Tc-pertechnectate uptake was observed at 1–3 h following transplantation of CDCs encapsulated in HA:Ser hydrogels (n=6, $p<0.001$) (Fig 2e, f), suggesting hydrogel-mediated in vivo restoration of cellular bioenergetics. The SPECT signal increased on d1–3 and was maintained for d7 post-transplantation (Fig 2f), indicating that HA:Ser hydrogels promote in vivo proliferation and short term engraftment following epicardial transplantation.

Intra-myocardial delivery of CDCs in HA:Ser hydrogels boosts acute retention and engraftment

Since acute stem cell retention in the myocardium following intra-myocardial delivery is low[3], effect of encapsulating CDCs in HA:Ser hydrogels on myocardial retention and cell bio-distribution was determined using ex vivo ^{18}FDG-labeled CDCs. Intra-myocardial injection of CDCs in suspension revealed retention of 12±4% of injected cells in non-infarcted hearts; encapsulation in HA:Ser hydrogels increased myocardial cell retention 6 fold (73±9%) and was associated with reciprocal reduction in lung retention (Fig 3a).

Next, serial in vivo BLI imaging using firefly luciferase-positive fLuc^{+}CDCs was performed to assess impact of HA:Ser hydrogels on engraftment following intra-myocardial transplantation. Injection of suspended CDCs led to progressive reduction in cell-derived signal over d7, whereas intra-myocardial injections of CDCs encapsulated in hydrogels led to 23% increase in cell-derived signal on d1 and maintenance of the signal over d7, indicating that intramyocardial transplantation of HA:Ser hydrogels promotes in vivo proliferation and short term engraftment (Fig 3b) of encapsulated stem cells.

Since reporter gene silencing can confound assessment of engraftment at >d7 post-transplantation, quantitative PCR analysis of the SRY gene was used to assess long term engraftment at d28 post-intramyocardial transplantation. Quantitative PCR[20] revealed 5 fold higher (p=0.03) d28 engraftment of CDCs encapsulated in HA:Ser hydrogels, when compared to suspended CDCs (Fig 3c).

HA:Ser hydrogels improve cardiac function post-MI and promote angiogenesis

Echocardiography was performed to evaluate effects of HA:Ser hydrogels on cardiac function post-MI. The following groups were studied in animals that underwent induction of myocardial infarction by ligation of the LAD: Placebo/Control (IMDM injection), intra-myocardial-CDC injection, intramyocardial-HA:Ser hydrogels, intramyocardial-HA:Ser hydrogels+CDCs and epicardial-HA:Ser hydrogels. An improvement in left ventricular ejection fraction (LVEF) was determined as relative increase in LVEF from d1 to d7 and d28 (Fig 3d). LVEF was unchanged in the control group (0.4±2%; n=6, p=0.8), increased by 8±6% (n=7, p=0.07) in the intra-myocardial CDC group, 13±4% (n=7, p<0.01) in the intramyocardial-HA:Ser group, 15±5% (n=7, p<0.01) in the intramyocardial-HA:Ser+CDC group, and 8±3% (n=6, p<0.01) in the epicardial-HA:Ser group at d28. Notably, epicardial or intramyocardial delivery of HA:Ser hydrogels were superior to placebo (p=0.012 for control versus HA:Ser intramyocardial; p=0.04 for control versus HA:Ser epicardial; p=0.01 for control versus HA:Ser intramyocardial +CDC) and similar to CDC delivery (p=0.4 for CDC vs HA:Ser intramyocardial; p=0.5 for CDC vs HA:Ser epicardial) at d28 post-MI.

Immunostaining for smooth muscle actin (SMA) and von Willebrand factor (vWF) was performed to assess myocardial vascularization induced by HA:Ser hydrogels without cells (Fig 4a). Here, angiogenesis was assessed following epicardial application of hydrogels to non-infarcted hearts to avoid the confounding effects of ischemia on angiogenesis[29, 30]. A 5–6 fold higher density of blood vessels was seen on d7, and 6–9 fold higher density on d14 following epicardial transplantation of HA:Ser hydrogels (Fig 4b), compared to control rats

(control and hydrogel treated rats had transient treatment with 2.5% trypsin- see methods). HA:Ser hydrogels are completely degraded in ~14 days in vivo.

Discussion

This is the first ever report of tissue engineered metabolic scaffolds. CDC encapsulation in HA:Ser hydrogels promotes rapid cell adhesion (integrin activation), increase in cellular glucose uptake and induces rapid restoration of cellular bioenergetics (Fig 4c), which lead to high viability of encapsulated stem cells, both in vitro and in vivo. Notably, cellular glucose and ^{99m}Tc-pertechnetate uptake as well as oxygen consumption (which reflect cellular metabolism) were markedly higher in HA:Ser hydrogels when compared to plating as monolayers (2D). The precise mechanisms whereby cell encapsulation in HA:Ser hydrogels leads to superior effects (compared to 2D monolayers) on metabolism is not known – it could involve access to greater numbers of adhesion sites or interplay between cytoskeletal changes induced by 3D encapsulation[31], serum-induced growth factor/integrin activation and activation of signaling pathways that regulate metabolism[31] by integrins and/or HA. Cells grown as monolayers are flat and spread in the horizontal plane, whereas suspended cells and cells encapsulated in hydrogels are spherical. The mechanism(s) whereby cytoskeletal changes influence cellular metabolism are not known, but could involve RhoA and Rac1, which are important regulators of actin cytoskeletal organization, cell-cell and cell-ECM adhesion, gene transcription, apoptosis and cell cycle progression[32, 33].

In vitro studies, in vivo SPECT imaging of NIS$^+$CDCs and in vivo BLI of fLuc$^+$CDCs indicate stimulation of encapsulated cell proliferation (Figs 1d, 2f, 3b) in HA:Ser hydrogels. The mechanisms underlying proliferation could be increased paracrine factor secretion by encapsulated cells (Fig 1e) and mitogenic effect of serum - these two effects could also potentiate HA-induced angiogenesis and stimulate functional recovery post-MI. Interestingly, cell proliferation assessed by SPECT and BLI peaked at 3 days and was reduced at 7 days post-transplantation (Figs 2f, 3b). Possible causes are reporter gene silencing and evolution of the infarct environment from the proliferative phase (d0–7 post-MI) to the reparative [34] or fibrotic (>d7 post-MI) phase. Inflammatory cells that infiltrate the infarcted region post-MI are known to secrete cytokines and growth factors that promote proliferation and activation of fibroblasts[34] – these paracrine factors could potentially promote proliferation of transplanted stem cells early following induction of myocardial infarction. Reduction in inflammation and growth factor/cytokine secretion during the reparative phase could contribute to reduction in transplanted cell proliferation in the hydrogel group and apoptosis[35] of the majority of transplanted cells in the control (non-hydrogel) group (Fig 3b).

HA:Ser hydrogels have the following features that make them good candidates for clinical translation: a) ease of synthesis; b) highly bio-adhesive: covalent cross-linking allows hydrogel synthesis and adhesion to beating hearts resulting in high rates of acute retention, without the use of ultraviolet light, heat or sutures; c) microenvironment that promotes rapid adhesion, survival and proliferation of encapsulated adult and embryonic stem cells; d) bio-degradable: degradation by enzymes such as hyaluronidases and proteases which are present in the heart, and by hydrolysis; e) HA and/or its degradation products promote

angiogenesis[36]; f) use of autologous serum would prevent immunogenic reactions and/or transmission of blood-borne diseases; g) HA:Ser hydrogels are porous, reflected by a high swelling ratio that permits delivery of systemically injected radiotracers/luciferin (Figs 2e, 3e) and would favor exchange of electrolytes, metabolites, substrates and permit cell migration. Importantly, animal mortality in this study was comparable to transplantation of suspended CDCs, in contrast to our previous studies where intra-myocardial injection of HA:lysed blood/serum hydrogels[11] or fibrin glue[3] led to ~100% mortality in treated animals. Since HA:Ser hydrogels adhere to beating hearts, they could be delivered intra-myocardially via injection catheters in the cardiac catheterization laboratory or applied to epicardium during open heart surgery.

The mechanism(s) underlying hydrogel-mediated functional improvement following MI is probably related to stimulation of angiogenesis (Fig 4). We found that functional benefit provided by HA:Ser hydrogels was similar to that provided by CDC-only transplantation (Fig 3d) – this is not surprising because functional benefit derived from adult stem cell transplantation is attributed primarily to paracrine factor secretion[18] and stimulation of angiogenesis. The HA and serum components of HA:Ser hydrogels could generate a ‘niche-like environment’ for stem cells by providing binding for CD44, CD169 and integrins which are expressed on stem cells and play important roles in adhesion/motility, gene expression, proliferation and signaling[8, 37, 38]. In support of this theory, we found that the microenvironment provided by HA:Ser hydrogels appears to be superior to the monolayer cell culture environment: paracrine factor expression (Fig 1e) and ^{18}FDG (Fig 2a) as well as ^{99m}Tc-pertechnetate uptake (Fig 2d) in hydrogels at 1 h and 24 h was markedly higher than with monolayer culture.

Currently, stem cell suspensions are frequently injected into the infarct border-zone[39–41] to improve their chances of cell survival following transplantation. Based on our results which indicate that CDCs survive and proliferate following epicardial delivery, HA:Ser hydrogels could be a good vehicle for stem cell transplantation into transmurally infarcted myocardium because they provide a microenvironment for cell survival, promote angiogenesis and attenuate infarct expansion (Fig 3f). HA:Ser hydrogel delivery into chronic, transmural infarcts are needed to evaluate impact of hydrogels on stem cell engraftment, dyskinetic wall motion and left ventricular remodeling[42].

Limitations

All in vivo and metabolism studies were performed using CDCs and HA:Ser hydrogels. Based on our in vitro studies, we anticipate that our results will be translatable to other stem cell types. Here, we used in vivo imaging rather than pathology to track stem cells - in vivo imaging precludes accurate localization of transplanted CDCs relative to the hydrogel due to limited spatial resolution of BLI and SPECT, but carries the advantage of permitting longitudinal investigation of in vivo stem cell biology. Here, reporter gene imaging was limited to 7 days because the cytomegalovirus (CMV) promoter is variably silenced in vivo after 7 days, which precludes accurate quantification of engraftment at longer time points. We did not compare HA:Ser hydrogels to commercially available agents such as fibrin glue because intra-myocardial injection of fibrin glue is lethal[3], probably due to activation of

the coagulation cascade; fibrin glue was also shown to increase mortality when used in patients during coronary bypass grafting[43]. Lastly, studies by other groups have demonstrated that HA-based hydrogels promote angiogenesis[44]; hence it is expected that HA:Ser hydrogels would also promote angiogenesis. The novel aspect of our study is the remarkable effect of HA:Ser hydrogels on bioenergetics and acute myocardial retention of encapsulated cells.

Conclusion

HA:Ser hydrogels contain adhesion motifs, that lead to rapid restoration of cellular metabolism, cell viability and proliferation. These metabolic scaffolds can be easily synthesized on site, injected intra-myocardially or applied epicardially, promote stem cell engraftment and angiogenesis, making them ideal candidates for clinical translation.

Acknowledgments

This work was funded by the American heart association (AHA-BGIA), NIH RO1 HL092985 and NIH 5UL1RR025005-05. Dr. Angel Chan was supported by NIH T32HL07227 Training Grant. Dr. Mehmet F. Karakas was supported by a TUBITAK 2219 Research Programme Grant (Scientific and Technological Research Council of Turkey-TUBITAK) and Fulbright Grant (Bureau of Educational and Cultural Affairs, United States Department of State). We are grateful to James Fox, Jim Engles, Karen Fox-Talbot and Gilbert Green for technical assistance.

References

1. Chang C, Chan A, Lin X, Higuchi T, Terrovitis J, Afzal JM, et al. Cellular bioenergetics is an important determinant of the molecular imaging signal derived from luciferase and the sodium-iodide symporter. Circ Res. 2013; 112:441–50. [PubMed: 23255420]
2. Makkar RR, Smith RR, Cheng K, Malliaras K, Thomson LE, Berman D, et al. Intracoronary cardiosphere-derived cells for heart regeneration after myocardial infarction (CADUCEUS): a prospective, randomised phase 1 trial. Lancet. 2012; 379:895–904. [PubMed: 22336189]
3. Terrovitis J, Lautamaki R, Bonios M, Fox J, Engles J, Yu J, et al. Non-invasive quantification and optimization of acute cell retention by in vivo positron emission tomography after intramyocardial cardiac-derived stem cell delivery. J Am Coll Cardiol. 2009; 54:1619–26. [PubMed: 19833262]
4. Hubbell JA. Bioactive biomaterials. Curr Opin Biotechnol. 1999; 10:123–9. [PubMed: 10209141]
5. Ferreira LS, Gerecht S, Fuller J, Shieh HF, Vunjak-Novakovic G, Langer R. Bioactive hydrogel scaffolds for controllable vascular differentiation of human embryonic stem cells. Biomaterials. 2007; 28:2706–17. [PubMed: 17346788]
6. Schussler O, Coirault C, Louis-Tisserand M, Al-Chare W, Oliviero P, Menard C, et al. Use of arginine-glycine-aspartic acid adhesion peptides coupled with a new collagen scaffold to engineer a myocardium-like tissue graft. Nat Clin Pract Cardiovasc Med. 2009; 6:240–9. [PubMed: 19234502]
7. Giancotti FG, Ruoslahti E. Integrin Signaling. Science. 1999; 285:1028–33. [PubMed: 10446041]
8. Gerecht S, Burdick JA, Ferreira LS, Townsend SA, Langer R, Vunjak-Novakovic G. Hyaluronic acid hydrogel for controlled self-renewal and differentiation of human embryonic stem cells. Proceedings of the National Academy of Sciences. 2007; 104:11298–303.
9. Toole BP. Hyaluronan in morphogenesis. Semin Cell Dev Biol. 2001; 12:79–87. [PubMed: 11292373]
10. Toole BP. Hyaluronan: from extracellular glue to pericellular cue. Nat Rev Cancer. 2004; 4:528–39. [PubMed: 15229478]
11. Chang CY, Chan AT, Armstrong PA, Luo HC, Higuchi T, Strehin IA, et al. Hyaluronic acid-human blood hydrogels for stem cell transplantation. Biomaterials. 2012; 33:8026–33. [PubMed: 22898181]

12. Strehin I, Nahas Z, Arora K, Nguyen T, Elisseeff J. A versatile pH sensitive chondroitin sulfate-PEG tissue adhesive and hydrogel. Biomaterials. 2010; 31:2788–97. [PubMed: 20047758]
13. Smith RR, Barile L, Cho HC, Leppo MK, Hare JM, Messina E, et al. Regenerative potential of cardiosphere-derived cells expanded from percutaneous endomyocardial biopsy specimens. Circulation. 2007; 115:896–908. [PubMed: 17283259]
14. Li TS, Cheng K, Malliaras K, Smith RR, Zhang Y, Sun B, et al. Direct comparison of different stem cell types and subpopulations reveals superior paracrine potency and myocardial repair efficacy with cardiosphere-derived cells. J Am Coll Cardiol. 2012; 59:942–53. [PubMed: 22381431]
15. Bonios M, Chang CY, Pinheiro A, Dimaano VL, Higuchi T, Melexopoulou C, et al. Cardiac Resynchronization by Cardiosphere-Derived Stem Cell Transplantation in an Experimental Model of Myocardial Infarction. Journal of the American Society of Echocardiography. 2011; 24:808–14. [PubMed: 21511432]
16. Barth AS, Kizana E, Smith RR, Terrovitis J, Dong P, Leppo MK, et al. Lentiviral Vectors Bearing the Cardiac Promoter of the Na+-Ca2+ Exchanger Report Cardiogenic Differentiation in Stem Cells. The American Society of Gene Therapy. 2008; 6:957–64.
17. Ahn SJ, Costa J, Emanuel JR. PicoGreen quantitation of DNA: effective evaluation of samples pre- or post-PCR. Nucleic Acids Res. 1996; 24:2623–5. [PubMed: 8692708]
18. Chimenti I, Smith RR, Li TS, Gerstenblith G, Messina E, Giacomello A, et al. Relative roles of direct regeneration versus paracrine effects of human cardiosphere-derived cells transplanted into infarcted mice. Circ Res. 2010; 106:971–80. [PubMed: 20110532]
19. Stastna M, Abraham MR, Van Eyk JE. Cardiac stem/progenitor cells, secreted proteins, and proteomics. FEBS Lett. 2009; 583:1800–7. Epub Mar 20. DOI: 10.016/j.febslet.2009.03.026 [PubMed: 19303873]
20. Bonios M, Terrovitis J, Chang CY, Engles JM, Higuchi T, Lautamaki R, et al. Myocardial substrate and route of administration determine acute cardiac retention and lung bio-distribution of cardiosphere-derived cells. J Nucl Cardiol. 2011; 18:443–50. [PubMed: 21448759]
21. Reid B, Afzal JM, McCartney AM, Abraham MR, O'Rourke B, Elisseeff JH. Enhanced tissue production through redox control in stem cell-laden hydrogels. Tissue Eng Part A. 2013; 19:2014–23. [PubMed: 23627869]
22. Bonios M, Chang CY, Terrovitis J, Pinheiro A, Barth A, Dong P, et al. Constitutive HIF-1alpha expression blunts the beneficial effects of cardiosphere-derived cell therapy in the heart by altering paracrine factor balance. J Cardiovasc Transl Res. 2011; 4:363–72. [PubMed: 21538185]
23. Fukushima S, Varela-Carver A, Coppen SR, Yamahara K, Felkin LE, Lee J, et al. Direct intramyocardial but not intracoronary injection of bone marrow cells induces ventricular arrhythmias in a rat chronic ischemic heart failure model. Circulation. 2007; 115:2254–61. [PubMed: 17438152]
24. Lozito TP, Jackson WM, Nesti LJ, Tuan RS. Human mesenchymal stem cells generate a distinct pericellular zone of MMP activities via binding of MMPs and secretion of high levels of TIMPs. Matrix Biol. 2014; 34:132–43. [PubMed: 24140982]
25. Chiarugi P, Giannoni E. Anoikis: A necessary death program for anchorage-dependent cells. Biochemical Pharmacology. 2008; 76:1352–64. [PubMed: 18708031]
26. Robey TE, Saiget MK, Reinecke H, Murry CE. Systems approaches to preventing transplanted cell death in cardiac repair. J Mol Cell Cardiol. 2008; 45:567–81. [PubMed: 18466917]
27. Shyh-Chang N, Daley GQ, Cantley LC. Stem cell metabolism in tissue development and aging. Development. 2013; 140:2535–47. [PubMed: 23715547]
28. Som P, Atkins HL, Bandoypadhyay D, Fowler JS, MacGregor RR, Matsui K, et al. A fluorinated glucose analog, 2-fluoro-2-deoxy-D-glucose (F-18): nontoxic tracer for rapid tumor detection. J Nucl Med. 1980; 21:670–5. [PubMed: 7391842]
29. Ware JA, Simons M. Angiogenesis in ischemic heart disease. Nature Medicine. 1997; 3:158–64.
30. Semenza GL. Hypoxia-inducible factor 1 and cardiovascular disease. Annu Rev Physiol. 2014; 76:39–56. [PubMed: 23988176]
31. Ochsner M, Textor M, Vogel V, Smith ML. Dimensionality controls cytoskeleton assembly and metabolism of fibroblast cells in response to rigidity and shape. PLoS One. 2010; 5:0009445.

32. Wang L, Yang L, Luo Y, Zheng Y. A novel strategy for specifically down-regulating individual Rho GTPase activity in tumor cells. J Biol Chem. 2003; 278:44617–25. Epub 2003 Aug 25. [PubMed: 12939257]
33. Heasman SJ, Ridley AJ. Mammalian Rho GTPases: new insights into their functions from in vivo studies. Nat Rev Mol Cell Biol. 2008; 9:690–701. DOI: 10.1038/nrm2476 [PubMed: 18719708]
34. Frangogiannis NG. The immune system and cardiac repair. Pharmacological Research: Pharmacology of Tissue Repair and Immunity in Regenerative Medicine. 2008; 58:88–111.
35. Hayakawa K, Takemura G, Kanoh M, Li Y, Koda M, Kawase Y, et al. Inhibition of granulation tissue cell apoptosis during the subacute stage of myocardial infarction improves cardiac remodeling and dysfunction at the chronic stage. Circulation. 2003; 108:104–9. [PubMed: 12821555]
36. Slevin M, Kumar S, Gaffney J. Angiogenic oligosaccharides of hyaluronan induce multiple signaling pathways affecting vascular endothelial cell mitogenic and wound healing responses. J Biol Chem. 2002; 277:41046–59. [PubMed: 12194965]
37. Hamilton SR, Fard SF, Paiwand FF, Tolg C, Veiseh M, Wang C, et al. The hyaluronan receptors CD44 and Rhamm (CD168) form complexes with ERK1,2 that sustain high basal motility in breast cancer cells. J Biol Chem. 2007; 282:16667–80. Epub 2007 Mar 28. [PubMed: 17392272]
38. Fujita Y, Kitagawa M, Nakamura S, Azuma K, Ishii G, Higashi M, et al. CD44 signaling through focal adhesion kinase and its anti-apoptotic effect. FEBS Lett. 2002; 528:101–8. [PubMed: 12297287]
39. Williams AR, Hare JM. Mesenchymal stem cells: biology, pathophysiology, translational findings, and therapeutic implications for cardiac disease. Circ Res. 2011; 109:923–40. [PubMed: 21960725]
40. Williams AR, Trachtenberg B, Velazquez DL, McNiece I, Altman P, Rouy D, et al. Intramyocardial stem cell injection in patients with ischemic cardiomyopathy: functional recovery and reverse remodeling. Circ Res. 2011; 108:792–6. [PubMed: 21415390]
41. Beeres SLMA, Bengel FM, Bartunek J, Atsma DE, Hill JM, Vanderheyden M, et al. Role of Imaging in Cardiac Stem Cell Therapy. Journal of the American College of Cardiology. 2007; 49:1137–48. [PubMed: 17367656]
42. Castelvecchio S, Menicanti L, Donato MD. Surgical Ventricular Restoration to Reverse Left Ventricular Remodeling. Curr. 2010; 6:15–23. DOI: 10.2174/157340310790231626
43. Goerler H, Oppelt P, Abel U, Haverich A. Safety of the use of Tissucol Duo S in cardiovascular surgery: retrospective analysis of 2149 patients after coronary artery bypass grafting. Eur J Cardiothorac Surg. 2007; 32:560–6. Epub 2007 Mar 23. [PubMed: 17363261]
44. Portalska KJ, Teixeira LM, Leijten JC, Jin R, van Blitterswijk C, de Boer J, et al. Boosting angiogenesis and functional vascularization in injectable dextran-hyaluronic acid hydrogels by endothelial-like mesenchymal stromal cells. Tissue Eng Part A. 2014; 20:819–29. [PubMed: 24070233]

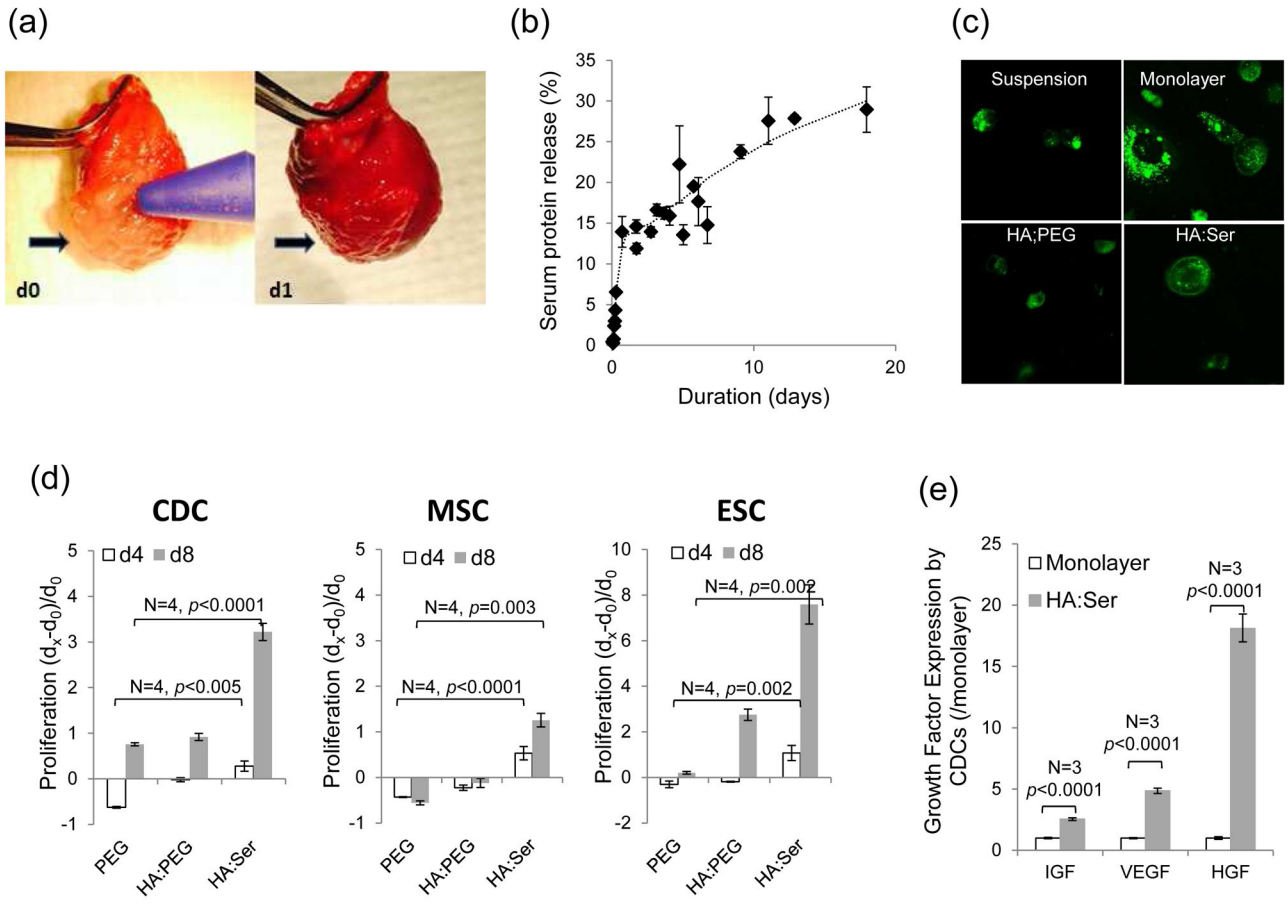

Fig 1.

(a) Epicardial application of HA:Ser hydrogels to beating hearts on d0 and d1. (b) Serum protein released profile from the hydrogel revealed ~5% serum released during the first 6 h after hydrogel synthesis, followed by a slower release over time, coincident with hydrogel degradation. (c) Two-photon microscopy revealed mainly cytoplasmic fluorescence in suspended CHO cells; prominent membrane localization of α_4 integrin-eGFP is seen within 1 h of encapsulating CHO cells in HA:Ser but not HA:PEG hydrogels. (d) Encapsulation in HA:Ser hydrogels promoted proliferation of CDCs, MSCs and ESCs, when assessed on d4 and d8 compared to d0, and higher proliferation compared to HA:PEG hydrogels (p<0.005). (e) IGF, VEGF, and HGF expression in CDCs encapsulated in HA:Ser hydrogels was significantly higher than CDCs cultured as monolayers (p<0.001).

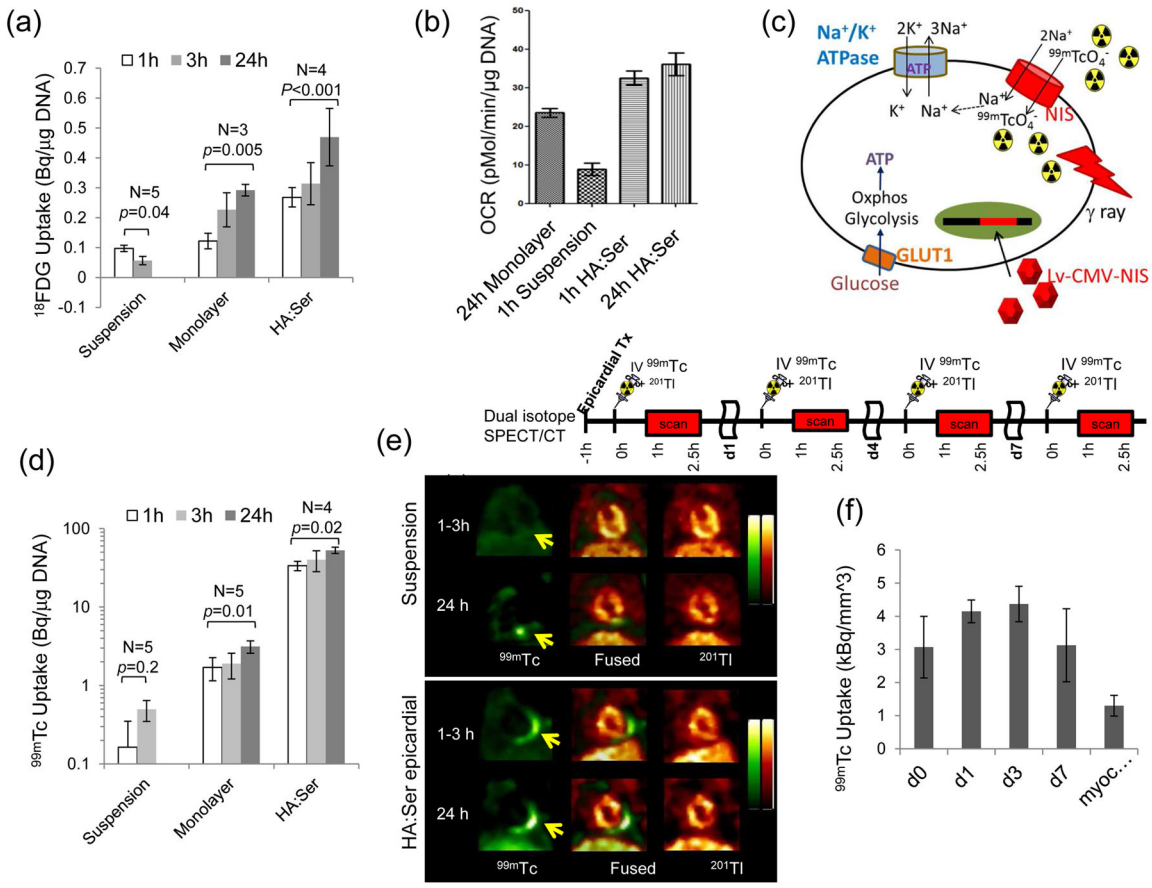

Fig 2.

(a) ^{18}FDG uptake in CDCs was markedly increased by encapsulation in HA:Ser hydrogels ($p \leq 0.005$). (b) CDC encapsulation restored oxygen consumption rate (OCR) within 1 h of CDC encapsulation. (c) Schematic illustrating link between ^{99m}Tc-pertechnetate uptake and Na^+-K^+- ATPase activity and metabolism. Oxphos: oxidative phosphorylation, GLUT-1: Glucose transporter-1, $^{99m}TCO_4^-$:^{99m}Tc-pertechnetate. (d) In vitro ^{99m}Tc-pertechnetate uptake in NIS$^+$CDCs was low in suspended CDCs and markedly increased within 1 h of encapsulation in HA:Ser hydrogels ($p<0.001$). (e) In vivo dual isotope SPECT-CT imaging showing ^{99m}Tc-pertechnetate uptake (yellow arrow) was low at 1–3 h following transplantation of suspended NIS$^+$CDCs (historic controls) and increased at 24 h post-transplantation. Encapsulation in HA:Ser hydrogels resulted in high ^{99m}Tc-pertechnetate uptake at 1–3 h and 24 h following transplantation (f) High in vivo ^{99m}Tc-pertechnectate uptake was observed at 1–3 h and maintained at d7 post-epicardial transplantation (n=4, $p<0.05$) of NIS$^+$CDCs encapsulated in HA:Ser hydrogels.

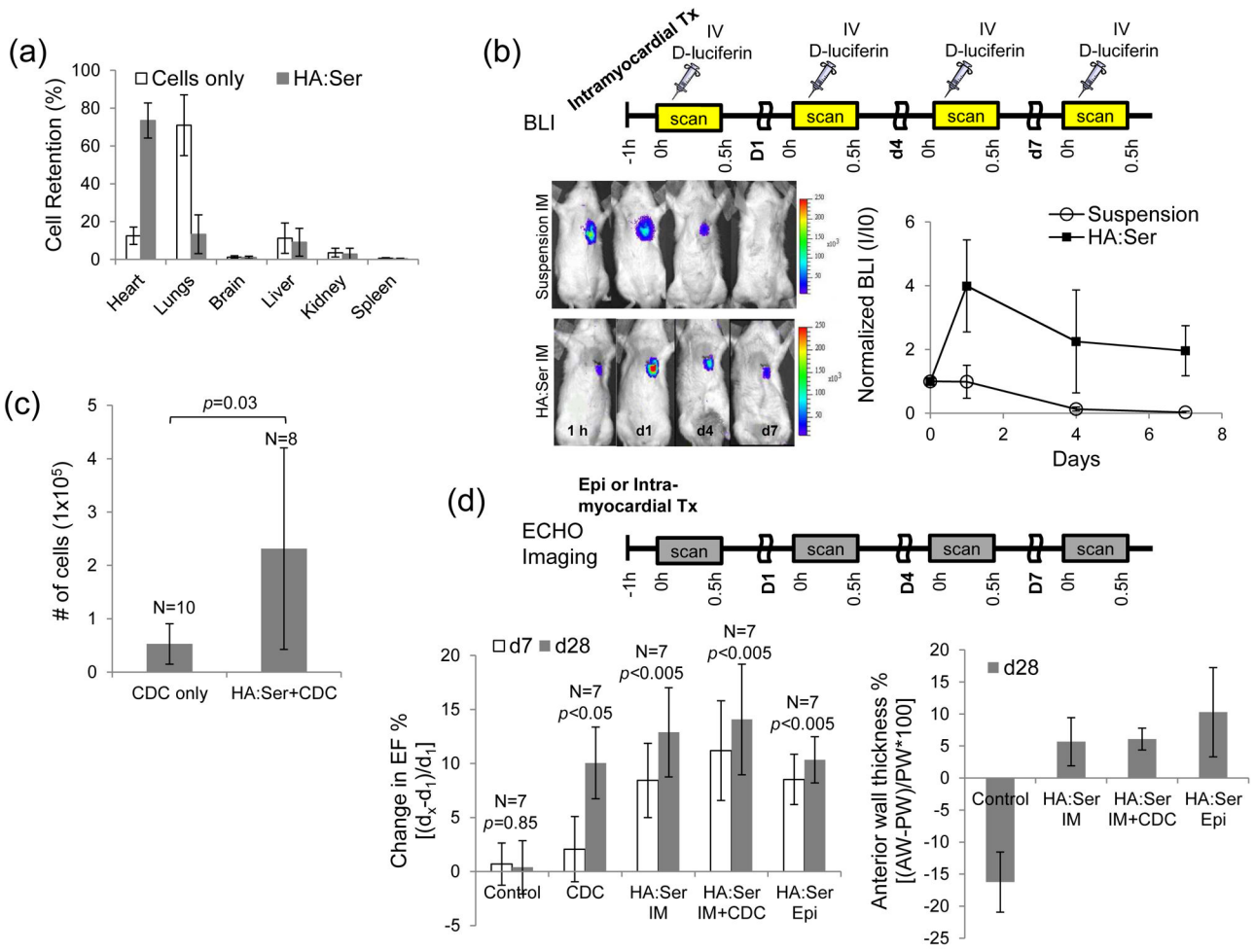

Fig 3.

(a) In vivo myocardial retention following intramyocardial injection of $^{18}FDG^{+}CDCs$: Encapsulation in HA:Ser hydrogels led to markedly higher acute myocardial retention at 1 h post-transplantation and lower cell egress into the lungs, when compared to cell suspensions ($p<0.001$). (b) In-vivo serial bioluminescence imaging of transplanted $fLuc^{+}CDCs$ for d7 revealed cell proliferation in the HA:Ser group and progressive cell loss in the suspension group; signal at each time point is normalized to d0 signal for the respective group. (c) CDC engraftment on d28 post-transplantation was significantly higher in HA:Ser groups when compared to transplantation of suspended CDCs. (d) Echocardiography revealed greater improvement in LVEF and infarct wall thickness in the CDC, intramyocardial HA:Ser, epicardial HA:Ser and intramyocardial HA:Ser+CDC groups compared to placebo.

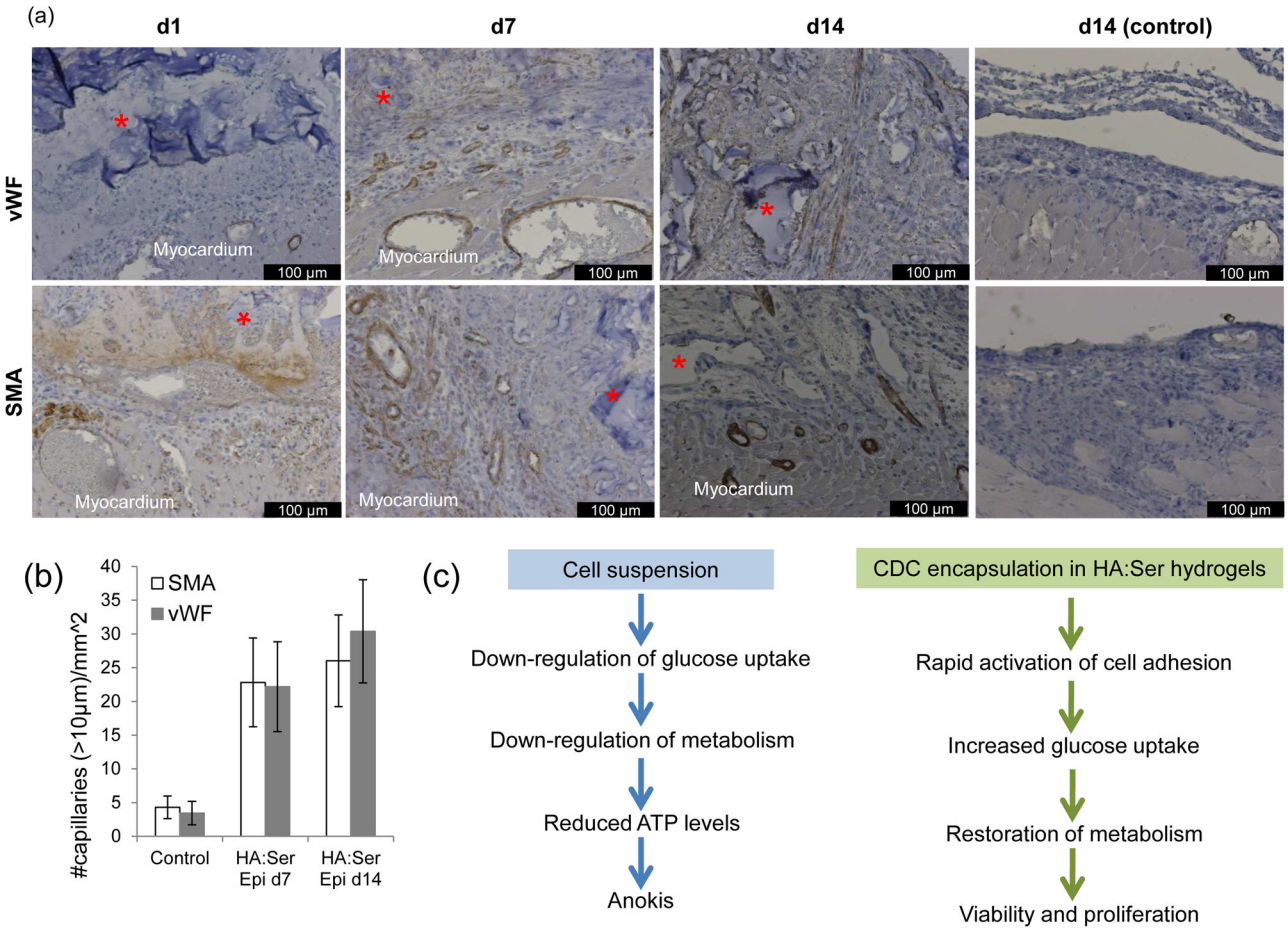

Fig 4.

(a) Immunostaining for vWF (top row) and SMA (bottom row) following epicardial application of HA:Ser hydrogel(*). On d1 after epicardial hydrogel application, engorgement of blood vessels in epicardial region was observed. Greater numbers of arteries and capillaries (arrows) were visible in the epicardial region and at the periphery of hydrogels on d7, and more organized blood vessels were seen within the transplanted HA:Ser hydrogels on d14 compared to controls on d14. (b) Epicardial application of HA:Ser hydrogels stimulates angiogenesis, detected by immunostaining for von Williebrand factor (vWF) and smooth muscle actin (SMA) (n=10, $p<0.001$). (c) Schematics illustrating effects of cell suspension and cell encapsulation in HA:Ser hydrogels on cellular bioenergetics and viability.